NJC

ROYAL SOCIETY OF CHEMISTRY

PAPER

View Article Online
View Journal | View Issue

Cite this: *New J. Chem.*, 2025, **49**, 11397

VTMS-based aerogel structure preservation: the influence of the sol–gel synthesis composition, aging process, and double-crosslinking

Aleksandra M. Pisarek, * Bartosz Nowak, Ryszard Jobda and Jakub M. Gac

Aerogels are highly porous materials that have a wide range of potential applications due to their exceptional properties – such as ultra-low density, high specific surface area, and low thermal and acoustic conductivity. One of the precursors gaining popularity in the aerogel synthesis is vinyltrimethoxysilane (VTMS) – due to the presence of the vinyl group which enables the modification of the aforementioned materials. However, VTMS still remains underexplored due to its synthesis challenges – such as frequent need for surfactants and difficulties in structure preservation during the ageing and drying processes. This study proposes a methodology for fabricating mesoporous VTMS-based aerogels *via* surfactant-free synthesis. The paper also identifies two primary mechanisms of structural degradation: dissolution during solvent exchange and shrinkage during aging and drying. The results indicate that the most effective way to prevent dissolution is the use of methanol in the solvent exchange process, which also eliminates cracks in the final aerogel structure. Shrinkage was found to be most effectively reduced by maintaining the sample in the mother liquor at an elevated temperature, while vulcanization proved to be an even more efficient method. Additionally, the study determines the synthesis compositions that enable the fabrication of the lowest-density aerogels.

Received 14th February 2025,
Accepted 2nd June 2025

DOI: 10.1039/d5nj00656b

rsc.li/njc

1. Introduction

The continuous development of technology requires new material solutions, in which aerogels play an essential role. Aerogels are highly porous materials (they can consist of up to 99.8% air), which translates into very low density (~0.003–0.5 g cm^{-3}).[1–3] Due to its often nanometer-sized dimensions, their open-pore structure results in a high specific surface area (500–1200 m^2 g^{-1}) and effective heat and energy management.[1–3] These properties contribute to their wide range of applications, including insulation (thermal, acoustic, or electrical), energy absorption, waste management, nuclear particle detection, catalysts and catalyst supports, pharmaceutical carrier materials, gas storage materials, batteries, and cosmic dust collectors.[4–10] It is worth noting that various aerogel properties may be crucial for fulfilling each application's requirements. At the same time, the final properties depend on the synthesis components and the final morphology of the obtained material.

Vinyltrimethoxysilane (VTMS) is an organoalkoxysilane precursor used to synthesize aerogels. Trifunctional organosilanes like VTMS can typically produce flexible aerogels with reduced bonding and enhanced hydrophobicity.[3] VTMS features three hydrolyzable alkoxy groups (which promote the growth of a silica network) and one polymerizable vinyl group. This reactive functionality enables further interactions with organic monomers, allowing the formation of hybrid aerogels where the oligomer component is effectively integrated into the silica structure, resulting in covalently bonded networks.[11] The VTMS precursor has also been explored as a grafting site to reinforce the silica aerogels with the polymer phase.[12]

In many studies, VTMS is used as a co-precursor (with compounds such as methyltrimethoxysilane – MTMS or tetramethyl orthosilicate – TMOS).[12–16] Its use as a single precursor remains limited, likely due to synthesis challenges related to the steric hindrance of the hydrophobic vinyl group, which hampers monolith formation. To avoid condensation issues associated with a vinyl group, a preliminary polymerization of VTMS has been proposed.[17–19] This approach converts vinyl groups into extended carbon chains, reducing the likelihood of phase separation or inhomogeneous reactions in solution. It is worth adding that while this method significantly enhances mechanical properties, it also removes the functional vinyl group, eliminating further modification options. In another approach, Shimizu *et al.* successfully synthesized single-precursor VTMS aerogels using a tailored surfactant system

Faculty of Chemical and Process Engineering, Warsaw University of Technology, Waryńskiego 1, 00-645 Warsaw, Poland.
E-mail: aleksandra.pisarek2.dokt@pw.edu.pl

(EH-208), which enabled the formation of flexible and translucent materials.[20,21] Vareda *et al.* demonstrated that VTMS-based aerogels can also be obtained without special alterations or the addition of extra substances, such as surfactants – offering a simpler and potentially more scalable alternative. However, the resulting product is limited to a macroporous material,[12] which, although having many advantages (*e.g.*, high elasticity), narrows the range of potential applications – particularly those requring a high specific surface area.

In addition to the still-discovered methods of synthesis and modification, the main disadvantage limiting the applicability of aerogels is the drying method. Obtaining an aerogel requires an exchange of the liquid present in the gel pores with gas without a skeleton collapse. This operation is challenging due to the high fragility of the 3D structure, consisting of randomly connected nanoparticles. To minimize the forces generated during drying by crossing the liquid–gas phase boundary, the primary technique used to obtain aerogels is supercritical drying (SCD). The SCD method prevents the pores from collapsing and receiving high-quality aerogels. However, SCD is an energy- and cost-consuming method that requires sophisticated equipment and is thus challenging to scale up.[22–24] A promising alternative in terms of investment and process cost is ambient pressure drying (APD). Nevertheless, a capillary pressure generated during the evaporation of liquid is destructive for a porous structure. As a result of the emerging forces, the pores collapse, and the entire structure undergoes significant shrinkage and cracking during the drying process.[2,3,22] Some authors have proposed counteracting the adverse effects of the APD method by using modification with a drying control agent (silylation).[24,25] Despite promising results, this method has drawbacks, such as introducing additional production steps and chemical alteration of the structure. Another way to use APD more widely may be through various silica network strengthening strategies. The strengthening can not only help to counteract the destructive pressures during drying but also enhance the mechanical resistance of the aerogel itself.

''Aging'' is a standard procedure used to strengthen the structure of the gel before it is dried. It involves additional cross-linking reactions and restructuring of the silica network (by thickening the necks between particles), which improves the mechanical stability of the material.[3,26] Although effective, conventional aging protocols include steps such as prolonged storage in the mother liquor or a specially prepared aging solution, temperature treatments, and solvent exchanges, often extending the process over several days or even weeks.[3,26–30]

The new paradigm in the literature on methods of strengthening organosilica aerogels is a process called vulcanization. This chemical modification, similar to vulcanization in silicone rubber materials, helps to produce aerogels with enhanced mechanical properties. Vulcanization is the post-gelation modification of the non-hydrolyzable vinyl group-containing structure (*e.g.* VTMS). After gelation, the vinyl groups remain in the porous structure, which makes it possible to polymerize them, thus forming double-crosslinking.[20] In this way, two types of bonds are present in the structure: ''standard'' siloxane bonds and carbon chains formed during polymerization. Vulcanization was indicated by the team of Shimizu *et al.* as a promising way to enhance Young's modulus and elasticity of samples.[20] The improved mechanical properties also significantly reduced volumetric shrinkage during drying using the cheap and scalable APD method. However, there are not many literature sources on this process, and there is still a lack of information on, among others, the influence of morphology on the effects of such modification.

This study focuses on developing a novel, surfactant-free method for synthesizing VTMS-based aerogels with a mesoporous structure, dried *via* ambient pressure drying (APD). The initial phase of the research involved synthesis optimization through the selection of alcohol and catalyst concentration. Subsequently, the effects of aging parameters – including temperature, time, and solvent – on the gel and aerogel structure were studied. Additionally, vulcanization was introduced as a secondary cross-linking strategy, to further reinforce the silica framework.

The resulting aerogels exhibited improved structural integrity and reduced shrinkage during ambient pressure drying. These findings provide valuable insights into how synthesis conditions and post-synthesis treatments influence the structure preservation of VTMS-derived aerogels. This study highlights the potential of combining an aging strategy and vulcanization to further limit volume shrinkage of aerogels produced using a cost-effective APD technique.

2. Experimental

2.1. Materials

Vinyltrimethoxysilane (VTMS) (98%), methanol (≥99.8%), *n*-butanol (≥99.4%), 2-propanol (≥99.5%), 2,2′-azobis (isobutyronitrile) (AIBN) (98%) were purchased from Sigma-Aldrich and used as received. Oxalic acid (98%) and aqueous tetramethylammonium hydroxide (TMAOH) (*ca.* 25%w), were also purchased from Sigma-Aldrich, but used as solutions in deionized water with the following concentrations: oxalic acid 0.2 M and TMAOH 2 M.

2.2. Preparation of VTMS gels

2.2.1. General synthesis procedure. Gels were synthesized using a two-step acid–base sol–gel method. The synthesis process began with mixing the appropriate amounts of VTMS and alcohol. The solution was stirred for 10 minutes, after which 0.2 M oxalic acid and a predetermined amount of water were added. The mixture was then stirred vigorously for one hour. Next, the stirring speed was reduced to prevent air bubble formation during gelation, and TMAOH (with concentration depending on the research section) was added to initiate condensation. The solution was then left undisturbed to gel. The entire synthesis was carried out at room temperature.

2.2.2. Solvent selection and TMAOH concentration adjustment. In the first section of the study, gels were prepared using two alcohols – methanol and *n*-butanol, two precursor

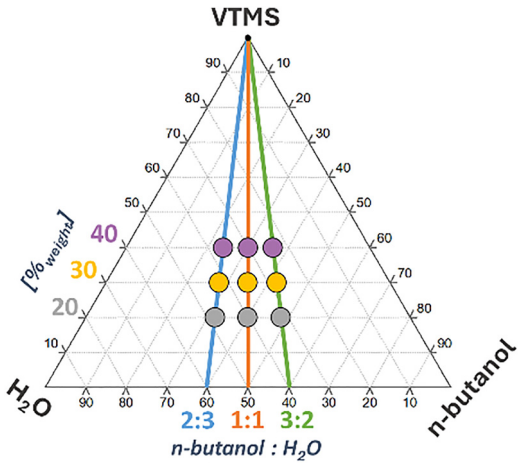

Fig. 1 Compositions of the syntheses used in the studies, presented as mass fractions on the pseudo-ternary system.

concentrations (20%$_w$ and 50%$_w$) and various concentrations of the basic catalyst TMAOH (in the range of 0.01–0.6 M in the entire mixture). A constant mass ratio of alcohol to water of 2 : 3 was maintained.

2.2.3. Synthesis compositions in structure preservation research. In subsequent sections, syntheses were performed with selected *n*-butanol as a solvent and a TMAOH concentration of 0.1 M (see details in Results and discussion). Nine synthesis compositions were used to investigate the effect of the aging and drying process, as marked in Fig. 1. The catalyst concentrations in the entire reaction mixture were kept constant for all samples: 0.002 M for oxalic acid and 0.1 M for TMAOH, which allowed considering the reaction mixture as a pseudo-three-component system (VTMS as a precursor, *n*-butanol as a solvent, and water as an antisolvent). The compositions were designed to differ in precursor concentration and alcohol-to-water ratio, as specified in Table 1.

2.3. Aging procedure

The aging process of variants and their respective conditions are summarized in Table 2. The first step of the aging process involved keeping the samples in the same container where gelation occurred (*i.e.* in the mother liquor). This step was conducted for a specified duration and temperature, as listed in Table 2. The next stage was solvent exchange, during which the samples were immersed in pure alcohol for 24 hours at room temperature. This procedure was repeated three times. In variants I and II, only 2-propanol was used, whereas in variants III and IV, the solvent was first replaced with methanol and subsequently with 2-propanol.

2.4. Vulcanization

Vulcanization was carried out on gels that had undergone the aging process marked as variant IV. A 0.05 M (8 g dm^{-3}) solution of AIBN, a radical polymerization initiator, was prepared in 2-propanol for this modification. The gel was than immersed in this solution (at a ratio of 5 mL of gel per 50 mL of solution). The vessel containing the sample was left at room temperature for 24 hours to ensure a homogeneous distribution of the initiator within the pore liquid. After this period, the container was transferred to 60 °C to initiate polymerization and maintained at this temperature for 48 hours. Finally, the solution containing the samples was cooled to room temperature, and the solvent was replaced with pure 2-propanol three times over 24 hours. The vulcanization methodology was established based on the work of Prof. Nakanishi's team.[20] The aging variant with additional vulcanization is marked as V.

Table 1 Volumes of individual synthesis components for a 5 mL sample

		Volume [mL]				
%VTMS$_w$	Alcohol : water (weight ratio)	VTMS	*n*-Butanol	Water	0.2 M Oxalic acid	2 M TMAOH
20	2 : 3	0.97	1.82	1.95	0.05	0.25
	1 : 1	0.95	2.24	1.55	0.05	0.25
	3 : 2	0.93	2.64	1.16	0.05	0.25
30	2 : 3	1.46	1.60	1.68	0.05	0.25
	1 : 1	1.43	1.97	1.33	0.05	0.25
	3 : 2	1.41	2.33	1.00	0.05	0.25
40	2 : 3	1.95	1.38	1.41	0.05	0.25
	1 : 1	1.93	1.70	1.11	0.05	0.25
	3 : 2	1.90	2.02	0.83	0.05	0.25

Table 2 Applied aging variants

	Time in mother liquor	Temperature during aging in mother liquor (°C)	Exchanging solvent
I	1 day	25	3× 2-propanol
II	1 day	50	3× 2-propanol
III	1 day	25	3× methanol, then 3× 2-propanol
IV	7 days	50	3× methanol, then 3× 2-propanol
V[a]	7 days	50	3× methanol, then 3× 2-propanol

[a] For variant V, vulcanization was additionally performed.

2.5. Ambient pressure drying

The gels were dried in a laboratory oven at atmospheric pressure. Drying was performed from pure 2-propanol, to which the liquid in the pores was replaced in the previous steps. During this stage, samples were placed for four to five days at 60 °C. Then, for one day, the temperature was increased to 80 °C to ensure that the remaining alcohol was removed from the pores.

2.6. Characterization

2.6.1. Visible-light transparency. The transparency of gels was evaluated using a UV-Vis spectrophotometer (Genesys 10S, Thermo Scientific). Transmittance of samples was measured for a wavelength λ = 550 nm. For this purpose, samples were gelled in polystyrene cuvettes (optical path = 10 mm).

2.6.2. Scanning electron microscopy observation. Ultra-high resolution scanning-transmission electron microscopy (SU8230, Hitachi) was utilized to observe the microstructure of the aerogels. The fragments of the samples (1–2 mm in size)

were placed on a dedicated mounting using carbon tape and then sputtered with a thin layer of gold using the Emitech K550X vacuum sputtering machine. Sample observation was carried out under the accelerating voltage of 15.0 kV.

2.6.3. Calculated parameters. One of the calculated values was the degree of conversion in the obtained aerogels. The conversion degree (α) has been computed as

$$\alpha = \frac{m_{\text{aerogel}}}{m_{\text{T}}} \tag{1}$$

m_{aerogel} denotes the mass of the aerogel for which the conversion degrees are determined, and m_{T} represents the theoretical mass assuming complete conversion of the precursor into vinylsilsesquioxane (VSQ) structures. This mass is calculated as

$$m_{\text{T}} = \frac{\text{conc}_{\text{VTMS}} \cdot \rho_{\text{VTMS}} \cdot V_{\text{VTMS}}}{M_{\text{VTMS}}} \cdot M_{\text{VSQ}} \tag{2}$$

where respectively: $\text{conc}_{\text{VTMS}}$ is the concentration of used VTMS solution (98%), ρ_{VTMS} – the density of the VTMS solution at room temperature (ρ_{VTMS} = 0.968 g cm^{-3}), V_{VTMS} – the volume of VTMS used in a specific synthesis, M_{VTMS} – the molar mass of VTMS (M_{VTMS} = 148.23 g mol^{-1}), and M_{VSQ} – the molar mass of vinylsilesquioxane (reacted VTMS to the siloxane network) (M_{VSQ} = 79.14 g mol^{-1}).

In this study, the apparent density (ρ_{gel}) and porosity (ε_{gel}) of the gel, as well as the density of the aerogel (ρ_{aerogel}) were also calculated using the following formulas:

$$\rho_{\text{gel}} = \frac{m_{\text{aerogel}}}{V_{\text{gel}}} \tag{3}$$

$$\varepsilon_{\text{gel}} = 1 - \frac{\rho_{\text{gel}}}{\rho_{\text{str.VTMS}}} \tag{4}$$

$$\rho_{\text{aerogel}} = \frac{m_{\text{aerogel}}}{V_{\text{aerogel}}} \tag{5}$$

where $\rho_{\text{str.VTMS}}$ is the structural density of VTMS, determined by helium pycnometry ($\rho_{\text{str.VTMS}}$ = 1.37 g cm^{-3}), and V_{gel} and *V*aerogel are the volumes of the gel and aerogel respectively.

Several quality parameters were used to assess the effectiveness of structure preservation methods. The first was the mass loss ($\%\text{ML}_{\text{aging}}$), which indicated the degree of dissolution. Mass loss was calculated using the following formula:

$$\%\text{ML}_{\text{aging}} = \frac{m_{\text{R}} - m_{\text{aerogel}}}{m_{\text{R}}} \tag{6}$$

where m_{R} is the mass of the reference aerogel. The reference aerogels were those obtained using the most effective aging method (variant IV), which resulted in the highest mass of obtained materials. It was assumed that no sample dissolution occurred in this series.

Another quality parameter – gel shrinkage during aging ($\%\text{VL}_{\text{aging}}$) was calculated as the volume loss:

$$\%\text{VL}_{\text{aging}} = \frac{V_{\text{gel,initial}} - V_{\text{gel,final}}}{V_{\text{gel,initial}}} \tag{7}$$

where $V_{\text{gel,initial}}$ denotes pre-aging gel volume and $V_{\text{gel,final}}$ – gel volume after this process.

To assess the impact of drying on structure preservation and compare it with the effect of aging, linear shrinkage (%LS) was calculated for each process:

$$\%\text{LS}_{\text{aging}} = \frac{d_{\text{gel,initial}} - d_{\text{gel,final}}}{d_{\text{gel,initial}}} \tag{8}$$

$$\%\text{LS}_{\text{drying}} = \frac{d_{\text{gel,final}} - d_{\text{aerogel}}}{d_{\text{aerogel}}} \tag{9}$$

where $d_{\text{gel,initial}}$ denotes pre-aging gel diameter, $d_{\text{gel,final}}$ – gel diameter after the aging process and d_{aerogel} is the diameter of the aerogel obtained after APD.

3. Results and discussion

3.1. Solvent selection and TMAOH concentration adjustment

Fig. 2A shows the gelation time, measured by the ''tilting'' method, for samples with different TMAOH concentrations, two precursor contents (20% and 50% weight fraction), and two alcohols used in the synthesis (methanol and *n*-butanol). The figure includes two graphs: one covering the full gelation time range (up to 20 hours), and the second graph – an enlargement of the time range from 0 to 25 minutes – to better illustrate differences in faster-gelling samples.

At low TMAOH concentrations (0–0.1 M), increasing catalyst content shortens gelation time. For samples synthesized in methanol: for 20%$_{\text{w}}$ VTMS (20%_MeOH) – gelation decreased from 5 minutes to 30 seconds, for 50%$_{\text{w}}$ VTMS (50%_MeOH) – from 2 minutes to 45 seconds, and for the 50%$_{\text{w}}$ VTMS sample synthesized in *n*-butanol (50%_*n*-BuOH) – from 15 minutes to 1.5 minutes. However, for the sample containing 20%$_{\text{w}}$ VTMS and synthesized in *n*-butanol (20%_*n*-BuOH), for the lowest TMAOH concentration used (0.01 M), a precipitate was formed. The minimum TMAOH concentration at which this sample gelled in the whole volume was 0.05 M, and when the concentration increased to 0.1 M, sample gelation time also increased (from 10 to 20 minutes).

A different trend was observed for TMAOH concentrations above 0.1 M. In this range (0.1–0.4 M), the gelation times increased with the catalyst concentration. For samples made using methanol, gelation times remained in the minute range: 30 seconds to 35 minutes (20%_MeOH) and from 1 to 12 minutes (50%_MeOH). However, the gels produced using *n*-butanol achieved a gelation time of even up to several dozen hours – for the 20%_*n*-BuOH sample, the gelation time in the TMAOH concentration range from 0.1 to 0.4 M increased from 20 minutes to 29 hours (except for the TMAOH concentration = 0.4 M, for which sample did not gel), and for 50%_*n*-BuOH sample – from 1 minute to 9.5 hours. In all cases, samples prepared with *n*-butanol gelled more slowly than those with methanol, and higher precursor content resulted in shorter gelation times.

Fig. 2B shows the light transmittance (λ = 550 nm) of the VTMS-based gels, measured *via* UV-Vis spectrophotometry. The

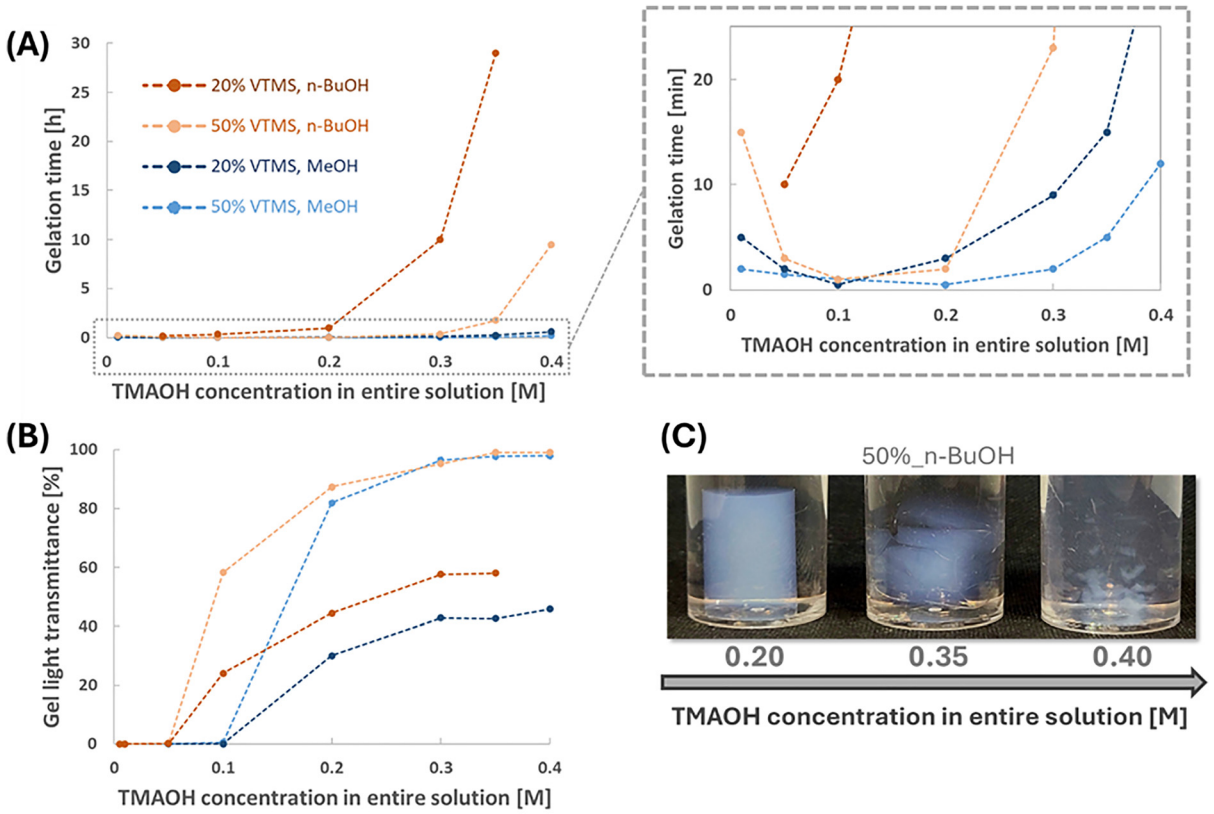

Fig. 2 (A) Gelation time for different TMAOH and VTMS concentrations and solvent types (with a detailed view of a particular period), (B) VTMS-based gels light transmittance for different TMAOH and VTMS concentration and solvent type, (C) Dissolution phenomenon depending on the TMAOH concentration.

methanol-based samples were opaque at 0.01–0.1 M TMAOH. Between 0.1 and 0.3 M TMAOH, transmittance increased with TMAOH concentration, stabilizing at 0.3–0.4 M TMAOH: ~44% for 20%_MeOH and ~97% for 50%_MeOH.

Meanwhile, for *n*-butanol-based gels, transmittance was nearly 0% at 0.01–0.05 M TMAOH. At 0.1 M TMAOH, it rose to ~24% (20%_*n*-BuOH) and ~58% (50%_*n*-BuOH), then further increased with catalyst concentration, reaching stable levels (~58% and ~98% respectively) at 0.3–0.4 M TMAOH. In nearly all cases, *n*-butanol samples exhibited higher light transmittance than methanol ones, except $50\%_w$ VTMS samples in the 0.3–0.4 M TMAOH concentration range, where transmittance was comparable for samples synthesized using both alcohols. Higher precursor content consistently led to greater optical clarity.

Fig. 2C presents photographs of 50%_*n*-BuOH samples synthesized using different TMAOH concentrations (0.2, 0.35, and 0.4 M) during solvent exchange (with 2-propanol at room temperature). The photographs show the dissolution phenomenon, which intensifies with increased TMAOH concentration. Preliminary observations indicate that this phenomenon is more pronounced in samples with lower precursor content.

The summary of results so far indicates that with increasing TMAOH concentration, the gelation time for most samples (except 20%_*n*-BuOH) first decreases with increasing base concentration in the range of 0–0.1 M, followed by an increase in the range of 0.1–0.4 M (Fig. 2A). This behaviour can be rationalized by considering the pH-dependent kinetics of condensation in sol–gel systems. According to Brinker and Scherer, the rate of condensation exhibits a non-linear dependence on pH, due to changes in the dominant reaction mechanism.[2,31–33] At low TMAOH concentrations (0–0.1 M), an increase in pH accelerates the relative rate of condensation, thereby shortening the gelation time. However, at higher base concentrations, the hydrolysis reactions become more promoted than condensation. Under strongly basic conditions (above pH ~10), the reactions reverse to condensation (*i.e.* hydrolysis and alcoholysis of siloxane bonds) also become more favourable.[20] Moreover, in such alkaline environments silica species are more likely to be ionized and therefore are mutually repulsive.[31]

In parallel, the observed increase in gel transparency with increasing TMAOH concentration can be attributed to the formation of smaller particles under high-pH conditions. The enhanced hydrolysis and alcoholysis at elevated pH reduce the degree of cross-linking, which limits the tendency toward phase separation. This, in turn, favours the development of a finer and more homogeneous network structure, resulting in reduced light scattering.[20] Additionally, another factors that may affect the transparency of the obtained gels include the

more homogenous network growth under slower, more controlled condensation, and the presence of the tetramethylammonium (TMA+) cation. Although not a classical surfactant, TMA+ may act as a structure-stabilizing agent by promoting better dispersion of hydrophobic species such as VTMS-derived intermediates. This effect likely contributes to the formation of structurally homogeneous and thus transparent gels.[34]

The choice of solvent had also a significant influence on both gelation time and the transparency of the obtained gels. Systems containing methanol gelled faster than those with *n*-butanol. This can be attributed to the higher polarity and lower steric hindrance of methanol, which increases the solubility of both VTMS and TMAOH, facilitates hydrolysis, and accelerates the formation of silanol groups.[35] In contrast, *n*-butanol has a lower polarity and longer alkyl chain, which reduces the miscibility of VTMS in the aqueous phase and slows down the hydrolysis–condensation process, resulting in longer gelation times.

Moreover, the difference in alcohol structure also affected the transparency of the final gels. Samples synthesized in *n*-butanol-based systems were generally more transparent. This can be attributed to the more gradual and controlled condensation process promoted by the lower polarity of the solvent, which favours the formation of a more homogeneous gel network. In addition, an increase in the alkyl chain length of the alcohol tends to reduce the pore size of the resulting gel network, which also contributes to improved transparency.[20]

The extended gelation time observed at lower precursor concentration can be attributed to the reduced number of hydrolyzable groups, which slows down the formation of the silica network. Additionally, as the precursor content decreases, the distance between reacting species increases, leading to lower collision frequency.[30,36,37] In contrast, a higher VTMS concentration provides more reactive sites and a shorter distance between reacting silica species, thereby promoting more uniform condensation and better dispersion. As a result, gels prepared with a higher precursor concentration exhibit enhanced transparency due to the increased structural homogeneity.[30,31]

Nevertheless, the dissolution of the gels may occur upon transferring them to pure 2-propanol for solvent exchange. Preliminary observations suggest that the extent of dissolution positively correlates with the increasing TMAOH concentration (Fig. 2C). This behaviour can be explained by the enhanced rate of reversible reactions under strongly basic conditions.[38,39] According to Brinker and Scherer, siloxane bonds (Si–O–Si) are susceptible to nucleophilic attack by hydroxide ions or alcohols, leading to network degradation through hydrolysis or alcoholysis, and ultimately dissolution of the silica framework.[31,33,35]

Based on the comprehensive observations, specific concentrations of TMAOH and types of alcohol were identified for further investigation. These criteria ensured a gelation time of no less than one minute, facilitating the synthesis process and optimizing transparency. A specific requirement was also established: complete dissolution must not occur at the chosen TMAOH concentration. In other words, following three solvent exchanges, gels obtained for both concentrations of VTMS should remain distinctly visible. These conditions were fulfilled with a TMAOH concentration of 0.1 M and the usage of *n*-butanol as a solvent. Therefore, these parameters were maintained for the subsequent phases of the research related to synthesis.

3.2. Influence of synthesis composition

After the initial selection of solvent and TMAOH concentration, the main set of samples was synthesized with variations in VTMS concentrations and alcohol : water mass ratios. Table 3 shows the degree of conversion, apparent density, and porosity for obtained VTMS-based gels.

The values represent properties of reference samples, *i.e.*, samples obtained by using a specific aging variant (variant IV) for which, after performing the solvent exchange, the highest aerogel masses were achieved (which indicated the lowest degree of solid phase dissolution). See the ''Effect of aging process'' section for the detailed difference in aging variants.

According to the data in Table 3, the conversion degree value increases with an increase in the precursor concentration. For samples with $20\%_w$ VTMS ranged from 71% to 79%; for samples with $30\%_w$ VTMS – 77% to 82%; and for samples with $40\%_w$ VTMS – 82% to 86%. Moreover, for most cases, as the alcohol : water ratio increases, the degree of conversion decreases. The average value of gels' apparent density and porosity for each precursor content shows a very low standard deviation (approximately 0.0055 g cm^{-3} and 0.4%, respectively), which indicates a marginal effect of the alcohol : water ratio.

Table 3 Conversion degree, density, porosity, and their standard deviations (SD) of investigated samples

$\%VTMS_w$	Alcohol : water (weight ratio)	Conversion $degree_r$ [%]	$Density_r$ [g cm^{-3}]	Average density [g cm^{-3}]	$SD_{density}$ [g cm^{-3}]	$Porosity_r$ [%]	Average porosity [%]	$SD_{porosity}$ [%]
20	2 : 3	77.01	0.0772	0.0762	0.0049	94.49	94.67	0.34
	1 : 1	78.77	0.0806			94.46		
	3 : 2	71.42	0.0709			95.06		
30	2 : 3	82.01	0.1238	0.1193	0.0065	91.16	91.54	0.41
	1 : 1	80.28	0.1223			91.48		
	3 : 2	76.79	0.1118			91.98		
40	2 : 3	86.46	0.1708	0.1655	0.0053	87.53	87.98	0.48
	1 : 1	84.86	0.1655			87.92		
	3 : 2	81.90	0.1603			88.49		

The calculated conversion degree values (based on dry gel' mass from variant IV, Table 3) increase with increasing the VTMS concentration and decreasing the alcohol : water ratio. This trend suggests that a higher precursor content, combined with lower solvent dilution, increases the concentration of reactive species in the sol, thereby enhancing the likelihood of their interaction and incorporation into the growing gel network. Additionally, a higher water content may increase the hydrolysis degree of methoxy groups, thereby amplifying the number of possible interconnections between molecules and promoting the formation of a more extensively crosslinked siloxane network.[30,33,37]

As the precursor concentration increases, both the mass and the volume of the resulting solid skeleton grow, leading to an increase in apparent density and a corresponding decrease in porosity. This indicates the formation of denser gel network, where the increased availability of reactive species promotes the development of a more tightly crosslinked silica framework.[30,40,41] Compared to precursor concentration, the alcohol-to-water ratio has a weaker influence on the final density and porosity (within the studied range).

Fig. 3A shows SEM images of the micromorphology of samples of nine synthesis compositions specified in Table 3. All obtained samples have a mesoporous structure. Based on SEM images, the sizes of secondary particles in each sample were measured. Fig. 3B shows an example of the dependence of the particle size distribution on the alcohol : water ratio (for a sample with 20%$_w$ VTMS). The smallest particle size was obtained for the alcohol : water ratio of 2 : 3 – the average particle size is 15 nm. With increasing alcohol content in the synthesis this size increases and for the ratio of 1 : 1 it is 30 nm, while for the ratio of 3 : 2 – 35 nm. Based on the results, it was noted that the average particle size increases with the increase of the alcohol : water ratio.

3.3. Effect of the aging process

For different aging variants (described in detail in the Experimental section), VTMS-based gels were compared in terms of mass and volume change – the comparison aimed to determine the effect of aging conditions on structure preservation during this stage. Mass loss qualitatively informs about the degree of structure dissolution, while volume loss informs about sample shrinkage caused by dissolution and syneresis – a process caused by the liquid expulsion from the pores, resulting in shrinkage of the gel network.[29] Fig. 4(A) and (E) show the loss of mass and volume due to aging, while Fig. 4(B–D) and (F–H) compare the specific aging variants by presenting the change in the mass and volume loss values.

Variant I, involving solvent exchange with 2-propanol at room temperature, served as the reference for comparing various structure preservation enhancement methods. As shown in Fig. 4A and E, this aging method led to the greatest structural degradation. Mass loss increased with precursor content: 63–69% for samples prepared with 20%$_w$ VTMS, to 37–40% for 30%$_w$, and 22–29% for 40%$_w$. The alcohol-to-water ratio also played a role: for 20%$_w$ VTMS, the highest mass loss was observed for the 1 : 1 ratio, and the lowest for 2 : 3. At higher precursor contents (30%$_w$ and 40%$_w$), the highest mass loss occurred for 3 : 2, and the lowest again for 2 : 3. Volume loss followed a similar trend but was consistently

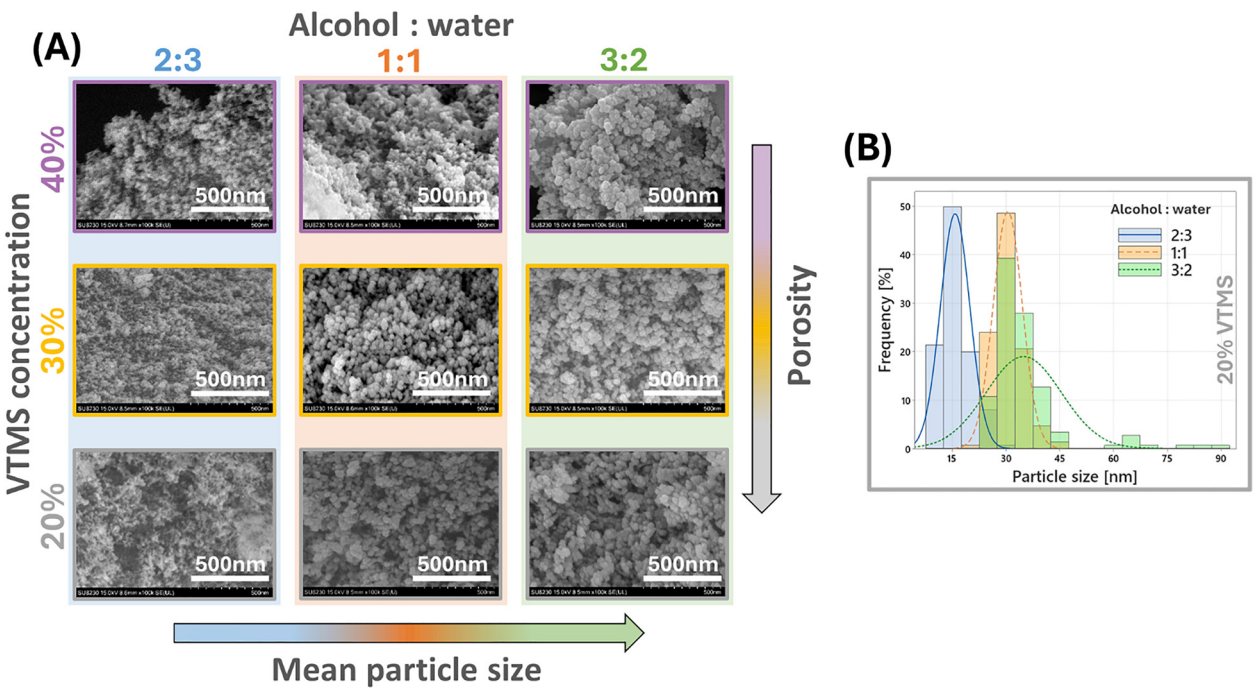

Fig. 3 (A) SEM images – approximated × 100k – of aerogels obtained from different synthesis compositions, (B) histogram of particle size distribution for samples with 20%$_w$ VTMS and different alcohol-to-water ratios in the synthesis.

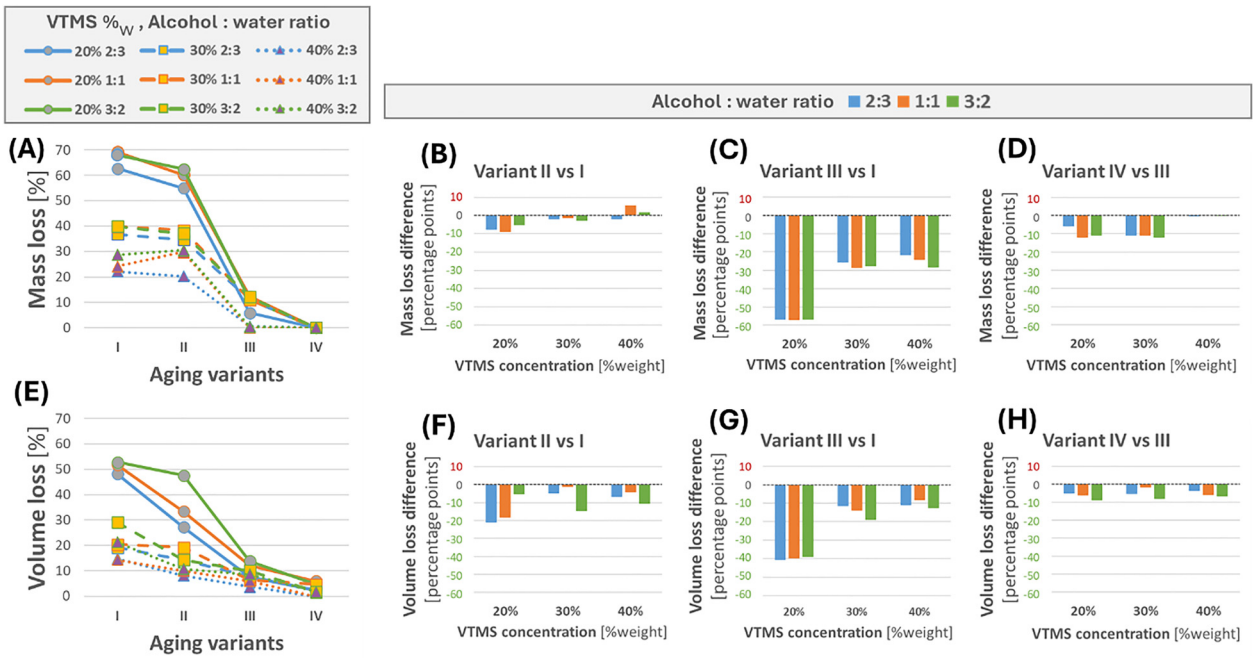

Fig. 4 (A) Mass loss during the aging process depending on the synthesis composition and the aging variant used, (B)–(D) difference in mass loss values for different synthesis compositions, between: variant II and I, III and I, and IV and III respectively, (E) volume loss during the aging process depending on the synthesis composition and the aging variant used, (F)–(H) difference in volume loss values for different synthesis compositions, between: variant II and I, III and I, IV and III respectively.

lower than mass loss. For 20%$_w$, 30%$_w$ and 40%$_w$ VTMS, the respective volume losses ranged between 48–53%, 19–29%, and 14–21%. For samples with all precursor contents, the greatest shrinkage occurred for the 3 : 2 ratio, while the smallest was observed 2 : 3 (except for 40%$_w$ VTMS, where it occurred for 1 : 1).

Variant II examined the effect of introducing elevated temperature during the sample's aging in the mother liquor. Fig. 4B and F show the changes in mass and volume loss (in percentage points (p.p.)) between the results from variant II and I. Reduction in mass loss can be observed for samples with the lowest precursor content (20%$_w$), on average by 7 p.p. For 30%$_w$ VTMS, no major change was observed – only 1–2 p.p., which is within the measurement error value. For the highest precursor content for alcohol : water ratios equal to 2 : 3 and 3 : 2, there was also no significant change (−2 and 2 p.p. respectively), while for the ratio 1 : 1, the sample dissolution increased – by 5 p.p.

In contrast, the introduction of elevated temperature during the aging in the mother liquor noticeably reduces the volume loss (more than the mass loss). The most significant shrinkage reduction was noted for the lowest precursor content (20%$_w$): by 18–21 p.p. for the 2 : 3 and 1 : 1 alcohol-to-water ratios, and by 5 p.p. for 3 : 2. For 30%$_w$ and 40%$_w$ VTMS, improvements mainly depended on the alcohol-to-water ratio: for 30%$_w$ VTMS, volume loss was reduced by 5, 1, and 15 p.p. for the 2 : 3, 1 : 1, and 3 : 2 ratios, respectively; while for 40%$_w$, respective reductions were 7, 4, and 11 p.p. Overall, the most significant structural losses – both in mass and volume – were observed for the lowest precursor content (20%$_w$) and the highest alcohol : water ratio (3 : 2).

Variant III aimed to investigate the effect of introducing an extra solvent exchange step with methanol. The results presented in Fig. 4C and G show a significant reduction in both mass and volume loss values. For the sample with a 20% precursor content, the difference in mass loss in the results of variants III and I reached up to 57 p.p. on average. A slightly lower reduction, but still significant, was achieved for samples with higher VTMS contents – for 30%, it was 26–29 p.p. and for 40%, from 22 to 28 p.p. Similarly, the largest decrease in volume loss (39–41 p.p.) was observed for the lowest VTMS content (20%). For samples with 30% of VTMS, the reduction in volume loss increases with the increasing alcohol content (12 p.p., 14 p.p. and 19 p.p. for alcohol : water ratio equal to 2 : 3, 1 : 1, and 3 : 2, respectively). Meanwhile, the 40% VTMS improvement in volume loss reduction is in the range of 8–13 p.p. Applying aging variant III leads to more significant dissolution reduction than shrinkage reduction for all investigated synthesis compositions. After aging using the method described in variant III, the samples with the lowest precursor content and the highest alcohol : water ratio continued (as in the other previously described variants) to exhibit the highest mass and volume loss values.

Variant IV builds upon variant III by incorporating methanol in the solvent exchange process and adding a 7-day aging period at an elevated temperature in the mother liquor. Fig. 4A illustrates that this variant's mass loss is 0% across all synthesis compositions. This result is based on the

assumption that the sample dissolution for variant IV is negligible, and the results from this aging method are used as the reference. The slight volume loss of the samples, as shown in Fig. 4E, does not exceed 6% for any of the samples, further supporting the no-dissolution assumption. Consequently, the remaining volume loss can be attributed to the syneresis phenomenon.

Comparing the results from variant IV and variant III, mass and volume loss reduction is visible. For lower precursor contents (20% and 30%), this improvement in the range is between 11 and 12 p.p., excluding the alcohol : water ratio of 2 : 3 for 20% VTMS, with a reduction of 6 p.p. This minor improvement results from the lowest mass loss obtained in variant III. Volume loss reductions increased with alcohol content for $20\%_w$ and $40\%_w$ VTMS (5–9 p.p. and 4–7 p.p., respectively). In the case of the samples with $30\%_w$ VTMS, there is no clear relationship between the alcohol : water ratio and the reduction of volume loss. For the 2 : 3 ratio, the reduction was 5 p.p., for 1 : 1 – 2 p.p., and for 3 : 2 – 8 p.p. Notably, while precursor content has a consistent effect on volume loss across variants (higher content = lower shrinkage), the influence of the alcohol-to-water ratio in variant IV was reversed compared to other variants. This may mean that samples with the highest alcohol : water ratio dissolve the most but shrink the least through syneresis.

Variations in mass and volume loss across aging variants influenced the final apparent density of the gels produced after the aging process (Fig. 5). Fig. 5B–D illustrate the relative changes in the density of the gels compared to their density after gelation.

As described above, the samples obtained from an aging variant I exhibit the highest degree of dissolution and shrinkage during aging. However, regardless of the precursor content and the alcohol-to-water ratios, the mass loss values are higher than the corresponding volume loss. This leads to decreased apparent density during aging across all synthesis compositions. Fig. 5A illustrates that, in many cases, the apparent density decreases more significantly for variant II of aging than for variant I. The elevated temperature utilized during the aging process in the mother liquor significantly reduced the shrinkage of the sample, with a lesser impact on dissolution. A minor change in the sample density was observed in variant III, which introduced methanol in the solvent exchange. Results suggest that changes in mass and volume balance each other. For samples with a VTMS concentration of 40%, a first-time increase in density was noted, which is linked to a significant decrease in gel dissolution. Variant IV is the variant in which 0% dissolution was assumed. However, some shrinkage still occurs for most samples, slightly increasing their apparent density.

In summary, elevated temperature during aging in mother liquor minimally reduces dissolution phenomena, and only for samples with the lowest precursor content. However, this method affects the reduction of volumetric shrinkage (for the sample with 20% VTMS and alcohol-to-water ratio 2 : 3 it was possible to reduce it by even 21 p.p.). This improvement can be attributed to an increased conversion degree of methoxy groups, as elevated temperature accelerates both hydrolysis and condensation rates.[26,28,31,35,42] Moreover, higher temperatures promote the dissolution and re-precipitation of soluble silica onto existing necks between particles, leading to thickening of the interparticle connections and, consequently, increased stiffness of the gel skeleton.[26,28,30,31,42] As a result, the more cross-linked and reinforced silica network becomes more resistant to deformation. Nevertheless, the limited impact on mass loss during aging suggests that thermal aging alone may not be sufficient to reinforce the structure. This is especially true considering that elevated temperatures, as previously noted, enhance the dissolution of silica and thereby can also contribute to network degradation during solvent exchange.

The second method of structure preservation – using methanol in solvent exchange – turns out to be much more efficient in reducing dissolution and shrinkage (than the method in variant II). Incorporating solvent exchange with methanol reduced

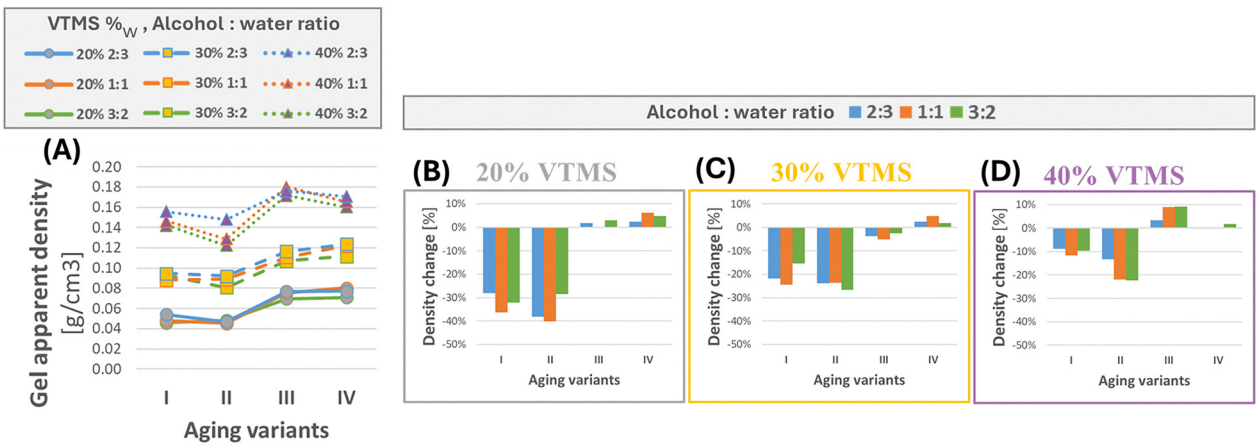

Fig. 5 (A) Apparent density of the gel after the aging process, depending on the synthesis composition and the aging variant, (B)–(D) change in apparent density of the gel during aging (compared to the gel after gelation), for different precursor concentrations: 20%, 30%, and 40% respectively.

mass loss by 22–57 p.p., while the loss of volume by 8–41 p.p. (depending on the composition used to synthesize the samples). This effect can be attributed to several factors. First, during the hydrolysis and condensation reactions of VTMS, methanol is generated as a by-product, meaning it is already present in the pore liquid immediately after gelation.[9,31] Introducing the same alcohol during solvent exchange ensures high miscibility and reduces the chemical potential gradient between phases, thereby minimizing osmotic stress and structural disruption.[30,43] Second, methanol has a lower viscosity and smaller molecular size that 2-propanol, which allows for faster and more uniform penetration into the gel network.[35,44] This facilitates a gentler and more homogeneous replacement of the pore fluid, which helps preserve the structural integrity of the gel. In contrast, direct solvent exchange with 2-propanol leads to greater structural disruption due to its slower diffusion rate and lower miscibility with the initial pore fluid, which generate stronger internal stresses. As a result, the solid network may become destabilized, causing partial detachment or collapse of the gel framework and leading to increased mass loss.

Nevertheless, the variant that most effectively enhances structure preservation during aging is variant IV, which combines the two aforementioned methods. For this variant, samples with the highest mass were obtained and shrunk by a maximum of 6% by volume. Regarding the apparent density of the gel, in variants I and II, where dissolution was most pronounced, a decrease in density was observed compared to the pre-aging gel. In contrast, in variants III and IV, the density increased slightly in most cases due to dissolution being reduced more effectively than shrinkage.

In studies of the synthesis composition effect on the dissolution and shrinkage, it was noted that the loss of mass and volume increases with the decrease in the precursor content and, in most cases, with the increase in the alcohol-to-water ratio. The effect of VTMS concentration may result from the decreasing degree of cross-linking for its lower concentrations, which is indicated by the degree of conversion (presented in Table 3). A lower degree of cross-linking implies a less integrated structure that is more susceptible to collapse or dissolution during solvent exchange. The effect of the alcohol-to-water ratio may result from several factors: (i) a decrease in the degree of cross-linking with lower water content, as indicated by the conversion values shown in Table 3; (ii) increased efficiency of dissolution of reprecipitation processes with increasing water concentration in the pores;[42] and (iii) various particle size distributions. The correlation of morphology with structure preservation requires additional studies. Still, one can speculate that variations in structural curvature might contribute to an increased degree of solid phase dissolution during solvent exchange, given that solubility is inherently related to the radius of curvature.[29] Samples with the highest alcohol-to-water ratio (3 : 2) have the largest average secondary particle size and the highest polydispersity index of size distribution (Fig. 3), which causes an increase in the curvature of the structure thus – may increase solubility.

3.4. Effect of the drying process

All samples subjected to aging using various variants were dried utilizing the ambient pressure method. Variant V marks samples subjected to vulcanization (see details in the Experimental section).

The impact of the aging method on structure preservation during the drying process was evaluated by measuring linear shrinkage, as indicated by changes in diameter, and by observing the formation of cracks in the structure of the dried gels. The alterations in diameter are presented in Fig. 6(A–F). In these graphs, the bars are divided into two segments: one segment corresponds to shrinkage resulting from aging (discussed in the preceding section), while the other segment pertains to shrinkage due to drying. Fig. 6(A–C) were generated with a constant alcohol-to-water ratio to investigate the effect of precursor concentration on diameter change. In contrast, Fig. 6(D–F) display similar results for a constant VTMS content ratio across various alcohol-to-water ratios.

In the case of variant I, drying-related shrinkage was similar for samples with 20% and 30% VTMS (49–52%) and slightly lower for 40% VTMS (42–43%), regardless of alcohol-to-water ratio. Moreover, Fig. 6G shows the total change in diameter (the sum of shrinkage due to aging and drying). Generally, total shrinkage decreases as precursor concentration increases and as the alcohol–water ratio decreases: 69–73% for 20% VTMS, 58–63% for 30%, and 48–49% for 40%. Additionally, Fig. 6H displays photographs of aerogel synthesized with a consistent composition (30% VTMS and an alcohol–water ratio of 2 : 3) but produced using different aging methods. It is evident that the aerogel obtained in aging variant I exhibited the most significant shrinkage and cracking.

Variant II, with one day of elevated-temperature aging in the mother liquor, resulted in similar or slightly higher shrinkage during drying (compared to results from variant I). For an alcohol-to-water ratio of 3 : 2, the relationship between precursor content and shrinkage remained consistent, but shrinkage values increased slightly. For 2 : 3 and 1 : 1 ratios, shrinkage during decreases with precursor content: 56% (20% VTMS), ~50% (30%), and 42% (40%). Total shrinkage followed trends similar to variant I but was slightly lower due to reduced aging shrinkage. Fig. 6H shows that both variant I and II samples are prone to cracking.

Methanol during the solvent exchange process in aging (variant III) did not help limit shrinkage *via* APD; in fact, it even increased shrinkage for samples with lower precursor content (20% and 30%). Another observation is that, after applying the aging described in variant III, the shrinkage during drying decreases as the concentration of VTMS in the synthesis increases, regardless of the alcohol-to-water ratio. For samples with 20% VTMS, the change in diameter ranges from 57% to 64%; for those with 30% VTMS 49–51%; and for 40% VTMS 41–43%. The shrinkage is not significantly influenced by the alcohol-to-water ratio, except for the sample with 20% VTMS, which exhibited greater shrinkage (64%) for a 1 : 1 ratio compared to other ratios (57–58%). However, using methanol

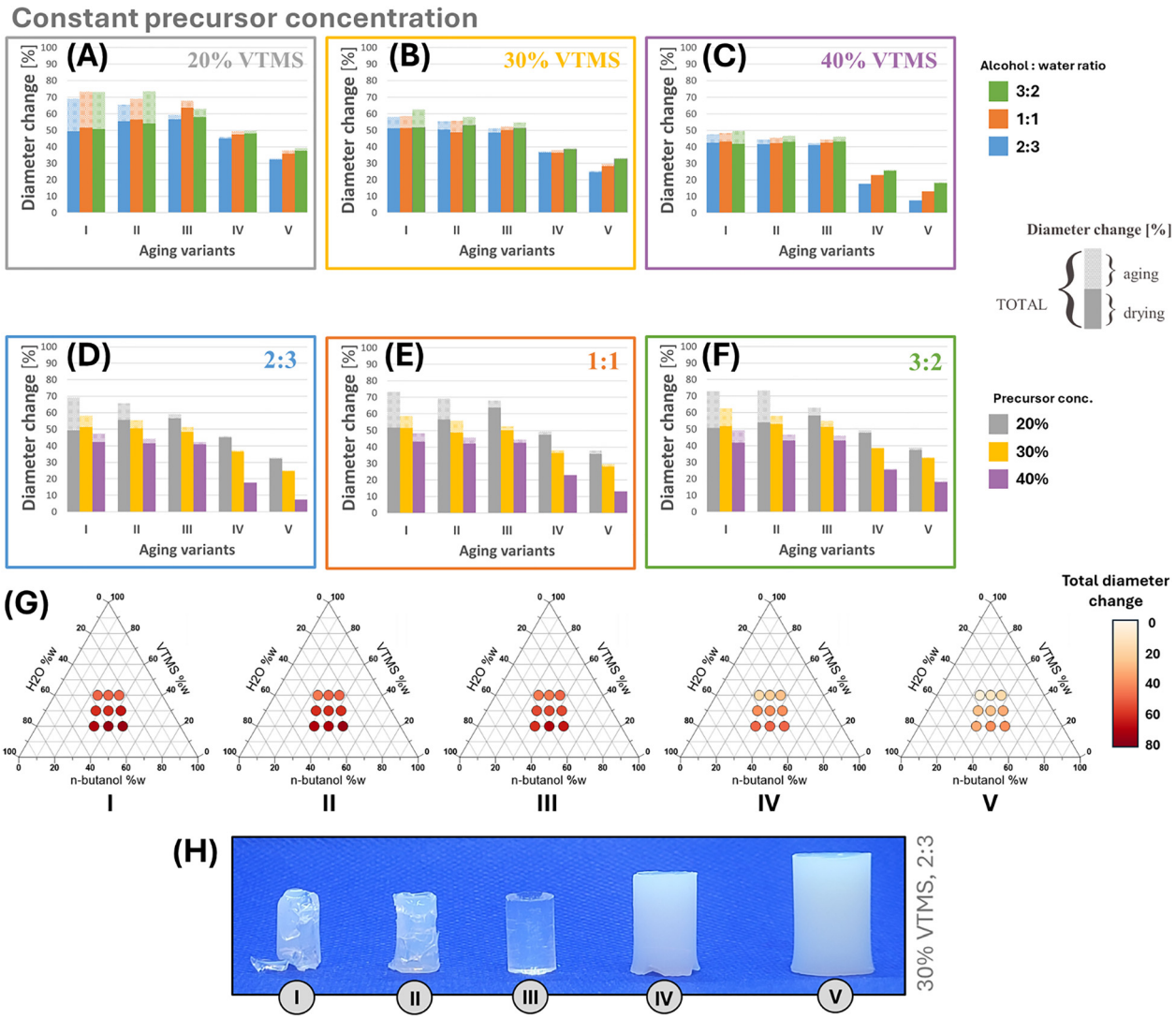

Fig. 6 (A)–(C) Change of diameter during aging and drying processes for different precursor contents: 20%, 30%, 40% respectively, (D)–(F) change of diameter during aging and drying processes for different alcohol-to-water ratios: 2 : 3, 1 : 1, 3 : 2 respectively, (G) total change of diameter between the sample after gelation and the obtained aerogel for different synthesis compositions presented in the ternary system, (H) photo showing aerogels obtained with 30% VTMS and alcohol-to-water ratio 2 : 3, using different aging variants.

in the solvent exchange process significantly reduced the shrinkage caused by aging. As a result, the total change in diameter is nearly identical to that caused only by drying. In samples with 20% precursor content, the total change in diameter is 3–5 percentage points greater than that caused by APD, while for samples with 30% and 40% precursor content, it is 1–3 percentage points greater. Despite the lack of improvement in shrinkage reduction with variant III, as illustrated in Fig. 6H, using methanol in the solvent exchange process helps eliminate cracks in the resulting aerogel.

The first significant reduction in diameter change is observed in variant IV, which involved using elevated temperatures in the mother liquor for 7 days and replacing the solvent with methanol. This combination of methods effectively minimizes structural shrinkage during drying, yielding better results than using either method alone. As with the previous variants, the degree of shrinkage during drying decreases as the VTMS concentration increases and the alcohol-to-water ratio decreases. Specifically, with 20% VTMS, the shrinkage values range from 45% to 48%; with 30% VTMS, it falls to between 36% and 39%; and with 40% VTMS, it further decreases to 18–26%.

In variant IV, the shrinkage during the aging process was minimal, resulting in the total diameter change being nearly equal to the change caused solely by drying. Analysis of Fig. 6H reveals a significant reduction in shrinkage due to this aging method compared to the previous variants. Additionally, no cracks were observed in the structure of the produced sample. However, a downside of this aging method is the decreased sample transparency.

The shrinkage values obtained from the samples produced using variant V indicate that vulcanization was the most

effective method for preserving the structure during drying. The diameter changes observed in these samples showed the lowest values compared to all other variants. In variant V, there was a noticeable decrease in shrinkage as the precursor content increased and the alcohol-to-water ratio decreased. For samples with 20% VTMS content, the shrinkage during drying varied with the increasing alcohol-to-water ratios (2 : 3, 1 : 1, 3 : 2) as follows: 32%, 36%, and 38%. The respective shrinkage values for samples with 30% VTMS were 25%, 28%, and 33%. In the case of samples with 40% VTMS, the shrinkage values were significantly lower at 8%, 13%, and 18%.

The photo presented in Fig. 6H illustrates that vulcanization successfully reduced shrinkage compared to variant IV. There were no visible cracks, and the transparency of the samples remained consistent.

The structural changes described above, including dissolution and shrinkage during aging and drying, significantly impact one of the aerogels' most crucial final properties: density. Fig. 7A presents the final density values of aerogels produced with various drying methods. Additionally, Fig. 7B through 7D illustrate how the density changes compared to the apparent density of the gel right after gelation, depending on the aging method used and the synthesis composition.

For variant I, it can be seen that the average value of aerogel density is the lowest for the sample with the highest precursor concentration (40%), and the highest for 30% VTMS. There is no clear relationship between the alcohol-to-water ratio and the density value. Moreover, variant I has some of the highest aerogel densities compared to other variants.

In most cases, increasing the temperature during gel aging in the mother liquor (variant II) led to a decrease in aerogel density compared to variant I. The only exception was the 20% VTMS sample with an alcohol-to-water ratio of 3 : 2, which exhibited a slight increase in density. The introduction of methanol in the solvent exchange process had little impact on aerogel density, as the values in variant III remained similar to those in variant I. Variant IV resulted in a significant reduction in the density of the aerogels. This effect was attributed to the combination of elevated temperature applied for seven days during aging in the mother liquor and the subsequent solvent exchange with methanol, effectively minimizing shrinkage during drying. Additionally, vulcanization contributed to the production of aerogels with the lowest densities. The lowest densities were observed for aerogels with a 40% precursor content, while the highest densities were recorded for 30% VTMS.

In summary, neither the use of elevated temperature during aging in the mother liquor nor the introduction of methanol in the solvent exchange led to significant changes in shrinkage during drying. However, applying an elevated temperature resulted in aerogels with lower density compared to variants I and III. This effect is due to the impact of this modification on the aging process – limiting volume loss while maintaining a high degree of dissolution. On the other hand, the use of methanol resulted in the elimination of cracks in the final aerogel structure and led to the highest transparency. This effect is consistent with the previously discussed role of methanol in stabilizing the gel structure during aging – its high miscibility and contribution to smoother solvent exchange likely helped reduce internal stress, thus preserving the integrity of the material.

A significant shrinkage reduction was achieved for aging variant IV (which consisted of a combination of the above-mentioned methods) and by using vulcanization. Variant IV reduced shrinkage by 1.5–2.7 times (depending on the sample composition) compared to the initial variant I. In comparison, vulcanization allowed the production of samples that shrank less by 1.8 to even 5.9 times. No cracks were observed in samples produced using these variants. However, their drawback is the reduced transparency of the obtained aerogels. Long aging at elevated temperature promotes extensive silica re-precipitation and thickening of interparticle necks, which, while beneficial for mechanical stability and shrinkage reduction, also leads to increases light scattering

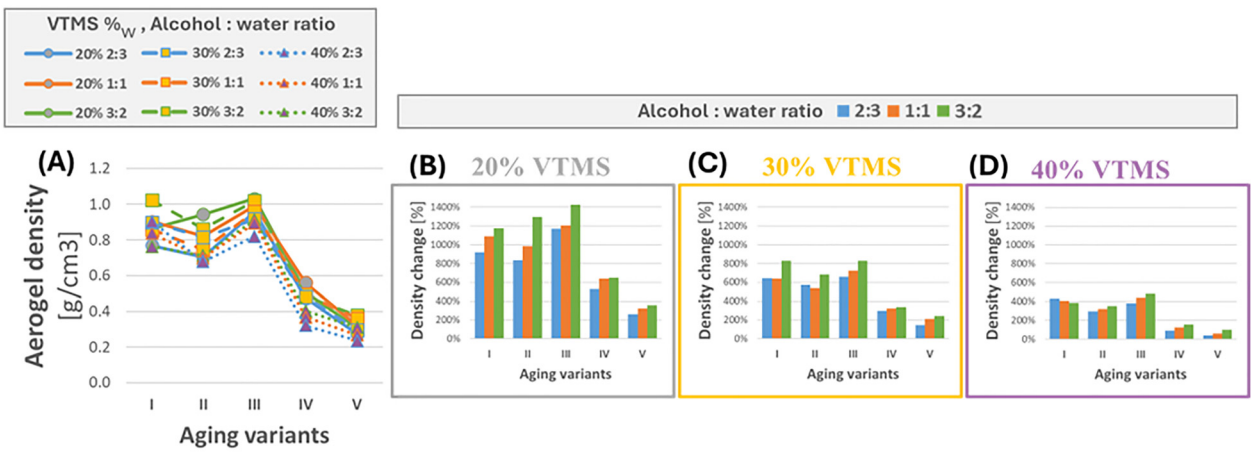

Fig. 7 (A) Apparent density of the obtained aerogels, depending on the synthesis composition and the aging variant, (B)–(D) change in density of aerogel compared to the gel after gelation, for different precursor concentrations: 20%, 30%, and 40% respectively.

due to the formation of larger or more interconnected particle domains.[30]

In all cases, the total shrinkage increases with decreasing precursor concentration and increasing alcohol-to-water ratio, which results in increased density. Consequently, unlike gels, aerogels with lower precursor content and higher alcohol content exhibited greater density. This shrinkage behaviour may be attributed to the degree of cross-linking, as indicated by the conversion degree (Table 3), as well as structural differences between samples – density of the samples after aging and the particle sizes in the gels. According to the relationship between Young's modulus and density,[45] samples with the lowest precursor content (20%) – and thus the lowest densities – likely have the weakest mechanical properties, leading to the highest shrinkage during APD. However, increasing the alcohol-to-water ratio results in larger particle sizes (Fig. 3), which at the same sample density may result in a smaller pore diameter. A smaller pore size, in turn, causes an increase in capillary pressure, which intensifies shrinkage.[22] In line with these findings, the lowest-density sample was the one synthesized with 40% VTMS and an alcohol-to-water ratio of 2 : 3, achieving a 0.236 g cm^{-3} density.

3.5. General trends – structure preservation

The results presented above reveal consistent relationships between synthesis parameters and the structural integrity of VTMS-based aerogels.

• Higher VTMS concentrations promote the formation of more extensively cross-linked networks, as indicated by higher conversion degrees (Table 3), leading to improved resistance to dissolution and shrinkage.[30,33,37,40,41] In contrast, lower precursor contents result in weaker structures that are more susceptible to degradation during solvent exchange and drying.

• The alcohol-to-water ratio influences reaction kinetics, morphology and the efficiency of dissolution and reprecipitation processes. The higher ratio limits hydrolysis due to reduced water availability, which lowers the degree of cross-linking (Table 3). It also leads to the formation of larger secondary particles and thus higher network curvature, which may increase degree of dissolution of solid framework.[31] Furthermore, a higher water content promotes the dissolution and subsequent reprecipitation of small silica particles at their contact points, enlarging the neck area and reinforcing the solid skeleton.[42]

• Aging at elevated temperature, enhances conversion degree of unreacted methoxy groups through accelerating hydrolysis and condensation rates, as well as silica reprecipitation onto interparticle necks. This improves stiffness and cohesion of the gel skeleton, making it more resistant to structure deformation (during aging and drying processes).[3,26,28,30,31,35,42]

• The solvent used during solvent exchange critically influences network stability. Methanol, being both a by-product of VTMS hydrolysis and condensation reactions, and a small molecule with low viscosity, enables smoother exchange. This reduces dissolution and helps maintain structural integrity and transparency in the obtained aerogel.[9,30,31,35,43,44]

• Vulcanization introduces a secondary cross-linking mechanism through the polymerization of vinyl groups. This leads to the formation of carbon chains embedded within the silica network, complementing siloxane bonding and significantly enhancing mechanical strength. Vulcanized gels exhibited the lowest shrinkage during drying with no cracking, confirming the effectiveness of the double-crosslinking strategy.[20]

Overall, structure preservation is governed by both chemical and physical factors: crosslinking degree, solvent compatibility, network curvature, and the presence of dual bonding mechanisms. The most effective stabilization was achieved by combining thermal aging, methanol exchange, and post-gelation vulcanization, resulting in robust, low-density, crack-free aerogels.

4. Conclusions

This work presents the development of a mesoporous, transparent, VTMS-based aerogel synthesis method without surfactant addition. Increasing the concentration of TMAOH (along with utilizing the *n*-butanol as a solvent) prolongs the gelation time and improves transparency. However, a higher TMAOH concentration also leads to increased dissolution of the gel samples during the solvent exchange stage.

The most effective strategy in terms of structure preservation combines solvent exchange with the methanol step with an extended aging time in the mother liquor at elevated temperature. Resulting in the least dissolved gels with volume shrinkage after aging limited to 6%. Furthermore, post-aging vulcanization proved to be the most effective approach in reducing linear shrinkage during APD – reducing it by nearly six times compared to the initial aging method.

Shrinkage observed during the drying process appears to be influenced by the density of the samples after aging and the mean particle sizes of the gels. As a result of these variables, the aerogels with the lowest final density, measuring 0.236 g cm^{-3}, were derived from samples (40% VTMS, alcohol-to-water ratio 2 : 3) that initially demonstrated the highest apparent gel density following gelation.

In terms of synthesis composition, the most significant structural changes during both aging and drying were observed in samples with the lowest precursor content (20%) and the highest alcohol-to-water ratio (3 : 2). It is suggested that the dissolution and shrinkage observed during aging may be related to the degree of cross-linking. Additionally, morphological differences might also influence these changes, but further studies are needed to establish specific relationships.

Author contributions

Aleksandra M. Pisarek: conceptualization; data curation; formal analysis; investigation; methodology; project administration; validation; visualization; writing – original draft. Bartosz

Nowak: conceptualization; formal analysis; writing – review & editing; Ryszard Jobda: investigation; validation; writing – review & editing. Jakub M. Gac: funding acquisition; resources; supervision; writing – review & editing.

Data availability

All data is included in the manuscript.

Conflicts of interest

There are no conflicts to declare.

Acknowledgements

This work was supported by the National Science Centre, Poland – project "Super-flexible double-crosslinked organosilica aerogels dried *via* cheap and scalable ambient pressure method" PRELUDIUM BIS (2021/43/O/ST8/01586).

References

1 S. S. Kistler, Coherent expanded aerogels and jellies, *Nature*, 1931, **127**(3211), 741.
2 N. Hüsing and U. Schubert, Aerogels—airy materials: chemistry, structure, and properties, *Angew. Chem., Int. Ed.*, 1998, **37**(1–2), 22–45.
3 H. Maleki and L. Durães, & A. Portugal, Synthesis of lightweight polymer-reinforced silica aerogels with improved mechanical and thermal insulation properties for space applications, *Microporous Mesoporous Mater.*, 2014, **197**, 116–129.
4 M. Schmidt and F. Schwertfeger, Applications for silica aerogel products, *J. Non-Cryst. Solids*, 1998, **225**, 364–368.
5 L. W. Hrubesh, Aerogel applications, *J. Non-Cryst. Solids*, 1998, **225**, 335–342.
6 J. L. Gurav, I. K. Jung, H. H. Park, E. S. Kang and D. Y. Nadargi, Silica aerogel: synthesis and applications, *J. Nanomater.*, 2010, **2010**(1), 409310.
7 Z. Mazrouei-Sebdani, H. Begum, S. Schoenwald, K. V. Horoshenkov and W. J. Malfait, A review on silica aerogel-based materials for acoustic applications, *J. Non-Cryst. Solids*, 2021, **562**, 120770.
8 G. Carlson, D. Lewis, K. McKinley, J. Richardson and T. Tillotson, Aerogel commercialization: technology, markets and costs, *J. Non-Cryst. Solids*, 1995, **186**, 372–379.
9 A. M. Anderson and M. K. Carroll, Hydrophobic silica aerogels: review of synthesis, properties and applications, *Aerogels Handb.*, 2011, 47–77.
10 A. C. Pierre and G. M. Pajonk, Chemistry of aerogels and their applications, *Chem. Rev.*, 2002, **102**(11), 4243–4266.
11 T. Matias, C. Varino, H. C. de Sousa, M. E. Braga, A. Portugal, J. F. Coelho and L. Duraes, Novel flexible, hybrid aerogels with vinyl-and methyltrimethoxysilane in the underlying silica structure, *J. Mater. Sci.*, 2016, **51**, 6781–6792.
12 J. P. Vareda, T. Matias and L. Durães, Facile preparation of ambient pressure dried aerogel-like monoliths with reduced shrinkage based on vinyl-modified silica networks, *Ceram. Int.*, 2018, **44**(14), 17453–17458.
13 B. N. Nguyen, M. A. B. Meador, M. E. Tousley, B. Shonkwiler, L. McCorkle, D. A. Scheiman and A. Palczer, Tailoring elastic properties of silica aerogels cross-linked with polystyrene, *ACS Appl. Mater. Interfaces*, 2009, **1**(3), 621–630.
14 H. Guo, B. N. Nguyen, L. S. McCorkle, B. Shonkwiler and M. A. B. Meador, Elastic low density aerogels derived from bis [3-(triethoxysilyl) propyl] disulfide, tetramethylorthosilicate and vinyltrimethoxysilane via a two-step process, *J. Mater. Chem.*, 2009, **19**(47), 9054–9062.
15 C. R. Ehgartner, S. Grandl, A. Feinle and N. Hüsing, Flexible organofunctional aerogels, *Dalton Trans.*, 2017, **46**(27), 8809–8817.
16 J. Y. Cai, S. Lucas, L. J. Wang and Y. Cao, Insulation properties of the monolithic and flexible aerogels prepared at ambient pressure, *Adv. Mater.*, 2011, **391–392**, 116–120.
17 G. Zu, K. Kanamori, T. Shimizu, Y. Zhu, A. Maeno, H. Kaji and J. Shen, Versatile double-cross-linking approach to transparent, machinable, supercompressible, highly bendable aerogel thermal superinsulators, *Chem. Mater.*, 2018, **30**(8), 2759–2770.
18 M. Fashandi, S. Karamikamkar, S. N. Leung, H. E. Naguib, J. Hong, B. Liang and C. B. Park, Synthesis, structures and properties of hydrophobic alkyltrimethoxysilane-polyvinyltrimethoxysilane hybrid aerogels with different alkyl chain lengths, *J. Colloid Interface Sci.*, 2022, **608**, 720–734.
19 S. Rezaei, A. Jalali, A. M. Zolali, M. Alshrah, S. Karamikamkar and C. B. Park, Robust, ultra-insulative and transparent polyethylene-based hybrid silica aerogel with a novel non-particulate structure, *J. Colloid Interface Sci.*, 2019, **548**, 206–216.
20 T. Shimizu, K. Kanamori, A. Maeno, H. Kaji, C. M. Doherty, P. Falcaro and K. Nakanishi, Transparent, highly insulating polyethyl-and polyvinylsilsesquioxane aerogels: mechanical improvements by vulcanization for ambient pressure drying, *Chem. Mater.*, 2016, **28**(19), 6860–6868.
21 T. Shimizu, K. Kanamori and K. Nakanishi, Transparent polyvinylsilsesquioxane aerogels: investigations on synthetic parameters and surface modification, *J. Sol-Gel Sci. Technol.*, 2017, **82**, 2–14.
22 A. Bisson, A. Rigacci, D. Lecomte, E. Rodier and P. Achard, Drying of silica gels to obtain aerogels: phenomenology and basic techniques, *Drying Technol.*, 2013, **21**(4), 593–628.
23 M. Shahzamani, R. Bagheri, M. Masoomi, M. Haghgoo and A. Dourani, Effect of drying method on the structure and porous texture of silica-polybutadiene hybrid gels: Supercritical vs. ambient pressure drying, *J. Non-Cryst. Solids*, 2017, **460**, 119–124.
24 N. Pawlik, B. Szpikowska-Sroka, A. Miros, B. Psiuk and A. Ślosarczyk, Effect of Drying Control Agent on

Physicochemical and Thermal Properties of Silica Aerogel Derived via Ambient Pressure Drying Process, *Energies*, 2023, **16**(17), 6244.

25 R. B. Torres, J. P. Vareda, A. Lamy-Mendes and L. Durães, Effect of different silylation agents on the properties of ambient pressure dried and supercritically dried vinyl-modified silica aerogels, *J. Supercrit. Fluids*, 2019, **147**, 81–89.

26 H. Omranpour and S. Motahari, Effects of processing conditions on silica aerogel during aging: Role of solvent, time and temperature, *J. Non-Cryst. Solids*, 2013, **379**, 7–11.

27 G. W. Scherer, Aging and drying of gels, *J. Non-Cryst. Solids*, 1988, **100**(1–3), 77–92.

28 S. Iswar, W. J. Malfait, S. Balog, F. Winnefeld, M. Lattuada and M. M. Koebel, Effect of aging on silica aerogel properties, *Microporous Mesoporous Mater.*, 2017, **241**, 293–302.

29 S. Ahmad, S. Ahmad and J. N. Sheikh, Silica centered aerogels as advanced functional material and their applications: a review, *J. Non-Cryst. Solids*, 2023, **611**, 122322.

30 O. Payanda Konuk, A. A. Alsuhile, H. Yousefzadeh, Z. Ulker, S. E. Bozbag, C. A. García-González and C. Erkey, The effect of synthesis conditions and process parameters on aerogel properties, *Front. Chem.*, 2023, **11**, 1294520.

31 C. J. Brinker and G. W. Scherer, *Sol-gel science: the physics and chemistry of sol-gel processing*, Academic press, 2013.

32 A. S. Dorcheh and M. H. Abbasi, Silica aerogel; synthesis, properties and characterization, *J. Mater. Process. Technol.*, 2008, **199**(1–3), 10–26.

33 N. H. Borzęcka, B. Nowak, J. M. Gac, T. Głaz and M. Bojarska, Kinetics of MTMS-based aerogel formation by the sol-gel method-experimental results and theoretical description, *J. Non-Cryst. Solids*, 2020, **547**, 120310.

34 R. Ueoka, Y. Hara, A. Maeno, H. Kaji, K. Nakanishi and K. Kanamori, Unusual flexibility of transparent poly (methylsilsesquioxane) aerogels by surfactant-induced mesoscopic fiber-like assembly, *Nat. Commun.*, 2024, **15**(1), 461.

35 A. A. Issa and A. S. Luyt, Kinetics of alkoxysilanes and organoalkoxysilanes polymerization: A review, *Polymers*, 2019, **11**(3), 537.

36 P. M. Shewale, A. V. Rao, J. L. Gurav and A. P. Rao, Synthesis and characterization of low density and hydrophobic silica aerogels dried at ambient pressure using sodium silicate precursor, *J. Porous Mater.*, 2009, **16**, 101–108.

37 D. Y. Nadargi and A. V. Rao, Methyltriethoxysilane: New precursor for synthesizing silica aerogels, *J. Alloys Compd.*, 2009, **467**(1–2), 397–404.

38 C. Sögaard, J. Funehag, M. Gergorić and Z. Abbas, The long term stability of silica nanoparticle gels in waters of different ionic compositions and pH values, *Colloids Surf., A*, 2018, **544**, 127–136.

39 G. B. Alexander, W. M. Heston and R. K. Iler, The solubility of amorphous silica in water, *J. Phys. Chem.*, 1954, **58**(6), 453–455.

40 B. Babiarczuk, B. Nowak, R. Mech, J. M. Gac, K. Kierzek, N. Borzęcka and J. Kaleta, Control of Structure and Mechanical Properties of Mtms-Based Aerogel Via Aqueous Catalyst Amount, Available at SSRN 5257611.

41 X. Deng, L. Wu, Y. Deng, S. Huang, M. Sun and X. Wang, … & Z. Li, Effects of precursor concentration on the physicochemical properties of ambient-pressure-dried MTES based aerogels with using pure water as the only solvent, *J. Sol-Gel Sci. Technol.*, 2021, **100**, 477–488.

42 F. He, H. Zhao, X. Qu, C. Zhang and W. Qiu, Modified aging process for silica aerogel, *J. Mater. Process. Technol.*, 2009, **209**(3), 1621–1626.

43 R. Subrahmanyam, P. Gurikov, P. Dieringer, M. Sun and I. Smirnova, On the road to biopolymer aerogels—Dealing with the solvent, *Gels*, 2015, **1**(2), 291–313.

44 D. W. Green, Perry's chemical engineers, *Handbook*, 2008.

45 M. Moner-Girona, A. Roig, E. Molins, E. Martınez and J. Esteve, Micromechanical properties of silica aerogels, *Appl. Phys. Lett.*, 1999, **75**(5), 653–655.